

1 **Abrupt climate and vegetation variability of eastern Anatolia during the last glacial**2 Nadine Pickarski^{1,*}, Ola Kwiecien², Dafna Langgut³, Thomas Litt¹3 ¹ *University of Bonn, Steinmann Institute for Geology, Mineralogy, and Paleontology, Bonn, Germany*4 ² *Ruhr-University Bochum, Sediment and Isotope Geology, Bochum, Germany*5 ³ *Tel Aviv University, Institute of Archaeology, Tel Aviv, Israel*

6 * Corresponding author. E-mail address: pickarski@uni-bonn.de

7 **Abstract**8 Detailed analyses of the Lake Van pollen, Ca/K ratio, and stable oxygen isotope record allow the
9 identification of millennial-scale vegetation and environmental changes in eastern Anatolia throughout the
10 last glacial (~111.5-11.7 ka BP). The climate of the last glacial was cold and dry, indicated by low
11 arboreal pollen (AP) levels. The driest and coldest period corresponds to Marine Isotope Stage (MIS) 2
12 (~28-14.5 ka BP), which was dominated by highest values of xerophytic steppe vegetation.13 Our high-resolution multi-proxy record shows rapid expansions and contractions of tree populations that
14 reflect variability in temperature and moisture availability. These rapid vegetation and environmental
15 changes can be related to the stadial-interstadial pattern of Dansgaard-Oeschger (DO) events as recorded
16 in the Greenland ice cores. Periods of reduced moisture availability were characterized by enhanced
17 occurrence of xerophytic species and high terrigenous input from the Lake Van catchment area.
18 Furthermore, the comparison with the marine realm reveals that the complex atmosphere-ocean interaction
19 can be explained by the strength and position of the westerlies, which are responsible for the supply of
20 humidity in eastern Anatolia. Influenced by the diverse topography of the Lake Van catchment, more
21 pronounced DO interstadials (e.g., DO 19, 17-16, 14, 12 and 8) show the strongest expansion of
22 temperate species within the last glacial. However, Heinrich events (HE), characterized by highest
23 concentrations of ice-rafted debris (IRD) in marine sediments, cannot be separated from other DO stadials
24 based on the vegetation composition in eastern Anatolia. In addition, this work is a first attempt to
25 establish a continuous microscopic charcoal record for the last glacial in the Near East. It documents an
26 immediate response to millennial-scale climate and environmental variability and enables us to shed light
27 on the history of fire activity during the last glacial.28 **1. Introduction**29 The last glacial inception was marked by the expansion of continental ice sheets and substantial changes
30 in oceanographic conditions in the North Atlantic as well as in atmospheric temperature and moisture
31 balance in the Northern Hemisphere (e.g., Blunier & Brook, 2001; Cacho et al., 2000, 1999; Chapman and
32 Shackleton, 1999; Rasmussen et al., 2014; Sánchez Goñi et al., 2002; Svensson et al., 2008, 2006; Wolff

33 et al., 2010). Between Marine Isotope Stages (MIS) 5d and 2, the climatic conditions were characterized
34 by numerous abrupt millennial-scale oscillations, known as Dansgaard-Oeschger events (DO; Dansgaard
35 et al., 1993). These are most prominently documented in Greenland ice cores and exhibit an abrupt
36 warming (Greenland interstadials; GI), followed by a gradual cooling and a final rapid temperature drop
37 towards a cold Greenland stadial (GS; e.g., NGRIP members, 2004; Rasmussen et al., 2014; Svensson et
38 al., 2008; Wolff et al., 2010). About 25 such stadial to interstadial transitions, varying in amplitude from
39 5°C to 16°C, are defined in the NGRIP record during the last glacial period (NGRIP members, 2004;
40 Rasmussen et al., 2014; Wolff et al., 2010). Although the climatic and environmental impacts of the DO
41 cycles have been intensively studied during the last decades, the mechanism behind them is still under
42 debate (e.g., Cacho et al., 2000, 1999; Rasmussen et al., 2014; Wolff et al., 2010). The main process
43 proposed as a cause for the recurring pattern is freshwater being forced from ice-sheets that affected the
44 extent of the sea ice, ocean heat transport, and Atlantic Meridional Overturning Circulation (AMOC;
45 Bond and Lotti, 1995; Cacho et al., 2000, 1999; Chapman and Shackleton, 1999; Hemming, 2004; Hodell
46 et al., 2008; McManus et al., 1999; Rasmussen et al., 2014; Wolff et al., 2010). The most extreme cold
47 intervals are Heinrich events (HE; Bond et al., 1993, 1992, Heinrich, 1988), characterized by reduced sea
48 surface temperatures (SST; Cacho et al., 1999) with highest concentrations of ice-rafted debris (IRD) in
49 marine sediments due to massive iceberg discharges, which mainly originated from the Laurentide ice
50 sheet (Alvarez-Solas and Ramstein, 2011).

51 Long-term terrestrial pollen records from the central and eastern Mediterranean, for example several crater
52 lakes in Italy (e.g., Lagaccione, Lago di Vico, Lazio Valle di Castiglione, Stracciacappa; Follieri et al.,
53 1998), Lago Grande di Monticchio (Italy; e.g., Allen et al., 1999), Lake Prespa (between Albania,
54 Republic of Macedonia, and Greece; Panagiotopoulos et al., 2014), Lake Ohrid (Albania; Lézine et al.,
55 2010) and Tenaghi Philippon (Greece; e.g., Müller et al., 2011) demonstrate a clear vegetation response to
56 millennial-scale climate variability during the last glacial. These regions are highly sensitive to short-term
57 vegetation changes as recognized by steppe-dominated open landscapes during stadials and increased
58 range of temperate tree taxa during interstadials (e.g., Allen et al., 2000, 1999; Follieri et al., 1998;
59 Langgut et al., 2011; Lézine et al., 2010; Müller et al., 2011; Panagiotopoulos et al., 2014; Shumilovskikh
60 et al., 2014). In contrast to southern Europe, high-resolution and continuous terrestrial sedimentary records
61 displaying abrupt climate oscillations are rare in the entire Near East.

62 Since the first long lacustrine sediment sequences were recovered at Lake Van in summer 2010 (Litt and
63 Anselmetti, 2014, Litt et al., 2012), numerous high-resolution data have been gathered, providing insight
64 into short-term changes in past climatic and environmental conditions in eastern Anatolia (e.g., XRF
65 measurements described by Kwiecien et al., 2014; total organic carbon content (TOC), Stockhecke et al.,
66 2014a). The sensitivity of this region was already well-documented by previous palynological data sets
67 covering the Late Glacial and the Holocene periods (Litt et al., 2009; Wick et al., 2003). First pollen

68 results of the new ~219 m long composite profile encompassing the last 600 ka, have been described
69 based on lower temporal resolution (between ~900 and 3,800 years) by Litt et al. (2014). A detailed high-
70 resolution pollen analysis (between ~100 and 800 years) for the last interglacial (131.2-111.5 ka BP) is
71 documented in Pickarski et al. (2015).

72 Here we present new biotic data (pollen, microscopic charcoal remains) and combine them with already
73 available Lake Van abiotic proxies (stable oxygen isotope and element measurements) of the last glacial
74 period (~111.5-11.7 ka BP). Special focus is given to the centennial- to millennial-scale climate
75 variability, as known from Greenland, and the regional response of vegetation to abrupt
76 paleoenvironmental changes in eastern Anatolia. After the examination of climate and vegetation changes
77 on a local level, we compare our results to selected global reference archives. Furthermore, we provide the
78 first continuous sedimentary microscopic charcoal record from Lake Van to give insights into the coupling
79 and feedback between fire activity and major changes in climate, vegetation, and fuel amount during the
80 last glacial.

81 **2. Regional setting**

82 Lake Van (38.6°N, 42.8°E) is a deep terminal alkaline lake (3,574 km²; max. depth >450 m) situated on
83 the eastern Anatolian high plateau at 1,647 m above sea level (asl, Fig. 1). It is the largest soda lake in the
84 world (Degens and Kurtman, 1978), which is partly fed by numerous small rivers around the basin. In the
85 south, the lake is surrounded by the Bitlis Massif reaching altitudes of more than 3,500 m asl. Two large
86 active stratovolcanoes, Nemrut (2,948 m asl) and Süphan (4,058 m asl), border the lake to the west and
87 north (Fig. 1B).

88 The present-day climate of eastern Anatolia is controlled by seasonal changes in the position and strength
89 of the following atmospheric components: (a) the mid-latitude westerlies, (b) the sub-tropical high-
90 pressure system, and (c) the Siberian high-pressure system (Akçar and Schlüchter, 2005; Türkeş, 1996).
91 The regional climate at Lake Van is continental with warm/dry summers (mean temperature >20°C;
92 Turkish State Meteorological Service) and cold/wet winters, marked by regular frosts. The minimum
93 average temperature of the coldest month is far below 0°C (-7.9°C in Van; see Fig. 1B for the location).
94 Total rainfall varies from 385 mm/a (Van) to 816 mm/a (Tatvan) and peaks in the winter months (October
95 to February), with a second rainfall maximum during spring (March to May). Higher elevations of the
96 west-east oriented mountain ranges along the Bitlis Massif (Fig. 1B) are affected by the strength and
97 position of the 'Cyprus cyclones' from the Mediterranean Sea with precipitation values up to 1,200 mm/a
98 in Bitlis (Turkish State Meteorological Service; Litt et al., 2014).

99 The modern distribution of vegetation at Lake Van is closely related to rough orography and spatial
100 rainfall variability. The southward slopes of the Bitlis Massif are covered by the Kurdo-Zagrosian oak
101 steppe-forest (*Quercetea brantii*), which extends from the Taurus Mountains (east-central Turkey) via the

102 Bitlis complex (SW shore of Lake Van) to the Zagros Mountains (SW Iran; Zohary, 1973). It consists of
 103 several oak species, which are accompanied by *Pistacia atlantica*, *P. khinjuk*, *Acer monsplessulanum*,
 104 *Juniperus oxycedrus*, *Pyrus syriaca*, *Crataegus* spp., *Prunus* and *Amygdalus* spp. (Frey and Kürschner,
 105 1989). In the rain-shadow, where rainfall decreases drastically, the northeastern part of the lake drainage is
 106 covered by Irano-Turanian steppe vegetation, dominated by *Artemisia fragrans*, steppe forbs and grasses
 107 (Zohary, 1973).

108 **3. Material and methods**

109 Sedimentary record 'AR' (Ahlat Ridge; 38.667°N, 42.669°E; 357 m water depth) was collected on a
 110 bathymetric ridge in the northern part of the Tatvan Basin (Fig. 1B) during the ICDP (International
 111 Continental Scientific Drilling Program) project PALEOVAN in summer 2010 (Litt and Anselmetti, 2014;
 112 Litt et al., 2012). Here we present data of the uppermost 3.87-41.72 m of the event-corrected composite
 113 record (mcblf-nE; depth scale, which excludes volcanic ash layers and mass flow deposits; Stockhecke et
 114 al., 2014a), representing the time span from 9.48 to 111.39 ka BP.

115 **3.1 Chronology**

116 The chronology of the Lake Van sedimentary sequence is based on an independent proxy records, e.g.,
 117 high-resolution XRF measurements (Kwiecien et al., 2014), total organic carbon (TOC; Stockhecke et al.,
 118 2014a), and pollen data (Litt et al., 2014), which were used for the construction of the age-depth model as
 119 published in Stockhecke et al. (2014a). By adding radiometric dating techniques, the Lake Van
 120 chronology was correlated by using 'age control points', derived from visual synchronization with the
 121 GICC05-based NGRIP isotope data for this relevant interval (0-116 ka; NGRIP members, 2004;
 122 Rasmussen et al., 2006; Svensson et al., 2008; Wolff et al., 2010). Additionally, a correlation with three
 123 $^{40}\text{Ar}/^{39}\text{Ar}$ dated onshore tephra layers was implemented in the age-depth model of the composite profile,
 124 i.e. the Nemrut Formation (NF) at 32.70 ± 2.55 ka BP, the Halepkalesi Pumice (HP-10) fallout at $61.60 \pm$
 125 2.55 ka BP as well as the Incekaya-Dibekli Tephra at ~ 80 ka BP (Stockhecke et al., 2014b; Sumita and
 126 Schmincke, 2013). Within the last glacial period, the palaeomagnetic Laschamp excursion at ~ 41 ka BP
 127 (Vigliotti et al., 2014) could be identified in the core sequence. Here we want to stress that, among data
 128 sets used for visual correlation, pollen data published in Litt et al. (2014) show the glacial/interglacial
 129 changes with the largest signal amplitude. However, the age-depth model of Stockhecke et al. (2014b) is
 130 based on tuning with the NGRIP event stratigraphy. The correlation points of the Lake Van sedimentary
 131 record have been mainly defined by abiotic proxies (i.e. TOC) caused by a higher time resolution of this
 132 data set in comparison to the pollen samples available during that time. Even if we present a high-
 133 resolution pollen record in this paper, leads and lags between different biotic and abiotic proxies related to
 134 climate events have to be taken into account.

135 **3.2. Palynology**

136 The new high-resolution palynological analyses were performed on 216 sub-samples taken at 10-20 cm
 137 intervals. The temporal resolution between each pollen sample, derived from the present age-depth model,
 138 is ranging from ~250 years (18.37-21.24 mcblf-nE) to ~500 years (3.87-18.37 and 21.24-41.72 mcblf-nE;
 139 Fig. 2).

140 Pollen samples were processed using standard palynological techniques (Faegri and Iversen, 1993)
 141 including chemical treatment with cold 10% HCL, hot 10% KOH, cold 40% HF, acetolysis and final
 142 sieving with 10 µm mesh size. In order to calculate the pollen and micro-charcoal (>20µm) concentrations
 143 (grains cm⁻³ and particles cm⁻³, respectively), tablets of *Lycopodium clavatum* (Batch No. 483216, Batch
 144 No. 177745) were added to each sample (Stockmarr, 1971).

145 Pollen identification was carried out to the possible lowest taxonomic level with reference of Beug (2004),
 146 Moore et al. (1991), Punt (1976), Reille (1999, 1998, 1995), and the pollen reference collections of the
 147 Steinmann-Institute, Department of Palaeobotany. Furthermore, we followed the taxonomic nomenclature
 148 after Berglund and Ralska-Jasiewiczowa (1986) and the detailed palynological investigation from the
 149 western Iran (van Zeist and Bottema, 1977).

150 To make these pollen counts statistically representative, a minimum of ~500 identified pollen grains per
 151 sub-sample were counted for the calculation of terrestrial pollen percentages (100%), composed of
 152 arboreal pollen (AP) and non-arboreal pollen (NAP). Spores of green algae (e.g., *Pediastrum boryanum*
 153 spp., *P. simplex*, *P. kawraiskyi*), dinoflagellate cysts, pollen grains of aquatic taxa and damaged pollen
 154 grains were excluded from the terrestrial pollen sum and pollen concentration. Percent calculation, cluster
 155 analysis to define pollen assemblage zones (PAZ), and construction of the pollen and charcoal diagram
 156 (Fig. 2) was carried out by using TILIA program; version 1.7.16 (© 1991-2011 Eric C. Grimm).

157 **3.3 Stable isotope analysis**

158 Lake Van carbonates consist of a mixture of calcite and aragonite precipitated in surface water. We
 159 selected 200 sub-samples at the same stratigraphic level which was used for the pollen analysis (20 cm
 160 sampling resolution). The freeze-dried and ground sediment samples were analyzed at the University of
 161 Kiel using a Finnigan GasBenchII with carbonate option coupled to a DELTAplusXL IRMS. The isotopic
 162 composition is given relative to the VPDB standard in the conventional δ -notation and was calibrated
 163 against two international reference standards (NBS19 and NBS18). The standard deviation for reference
 164 analyses was 0.06 ‰ for the stable isotope signature.

165 **3.4 Profiling measurements**

166 Profiling measurements of the complete Lake Van sedimentary record (Ahlat Ridge site) are published
 167 and described in detail by Kwiecien et al. (2014) as well as in the high-resolution study of the last
 168 interglacial by Pickarski et al. (2015).

169 The sediment cores were scanned with an AVAATECH XRF Core Scanner III at MARUM (Bremen).
 170 Intensities of major elements (e.g., Ca, K) on sediment cores were collected every 2 cm down-core over a
 171 1 cm² area. The row XRF measurements were processed by the Iterative Least square software (WIN
 172 AXIL) package from Canberra Eurisys, providing intensity data in total counts (tc). The Ca/K ratio
 173 presented in this paper is unitless.

174 **4. Results**

175 **4.1. Palynology**

176 The palynological data of the last glacial are presented in Fig. 2. This sequence can be divided into four
 177 pollen assemblage superzones (PAS IIa, IIb, IIIa, IIIb) following the criteria described in Tzedakis (1994
 178 and references therein), which were applied in Litt et al. (2014) for the low-resolution 600 ka long Lake
 179 Van pollen record. The PAS IIa and IIb can be further subdivided into six pollen assemblage zones (PAZ;
 180 Fig. 2) based on changes in the AP/NAP ratio and changes in the relative frequency of individual taxa.
 181 Main characteristics of each pollen zone and sub-zone as well as criteria for defining the lower boundaries
 182 are given in Table 1.

183 The pollen concentration varies between ~2,000 and 40,000 grains cm⁻³ dominated by steppic herbaceous
 184 pollen types in particular by *Artemisia* (5-55%), *Chenopodiaceae* (3-64%), and *Poaceae* (6-35%). Total
 185 arboreal pollen percentages alternate between 0.5 and 67% during the last glacial. The main tree taxa are
 186 *Pinus* (0-61%) and deciduous *Quercus* (0-15%), whereby the most indicative temperate taxon is
 187 deciduous *Quercus* characterized by relative high percentages during interstadials.

188 Microscopic charcoal concentrations vary between <200 and ~15,000 particles cm⁻³ throughout the last
 189 glacial (Fig. 2, 3D). In general, charcoal particles of a size commonly recorded from pollen slides reflect
 190 fire on a more regional scale (e.g., Clark et al., 1998; Tinner et al., 1998). Here the Lake Van charcoal
 191 record can be divided into two distinct intervals: (I) the glacial/stadial interval, when global temperatures
 192 and terrestrial biomass were relative low, the charcoal particles concentration stay low (<1,000 particles
 193 cm⁻³), and (II) the early interglacial/interstadial interval, when global temperatures increased and
 194 vegetation changed, the charcoal record shows high concentrations (>1,000 particles cm⁻³).

195 **4.2. $\delta^{18}\text{O}_{\text{bulk}}$ and XRF**

196 The oxygen isotopic composition of bulk sediments ($\delta^{18}\text{O}_{\text{bulk}}$) reflects regional climate changes and local
 197 temperature variability. However, the interpretation of $\delta^{18}\text{O}_{\text{bulk}}$ is complex as it can be influenced by a
 198 number of climate variables, such as air and water temperature, seasonality of precipitation, moisture

199 source and precipitation-to-evaporation ratio. According to Litt et al. (2012, 2009) and Lemcke and Sturm
 200 (*1997*), the $\delta^{18}\text{O}_{\text{bulk}}$ values of carbonates at Lake Van are primarily controlled by evaporation processes.
 201 Furthermore, Kwiecien et al. (2014) and Pickarski et al. (2015) mention that changes in seasonal rainfall
 202 have a significant effect on lake water isotope values. During the last glacial, the oxygen isotope signature
 203 of carbonates was apparently heavier during interstadials and lighter during stadials (Fig. 3B).
 204 The presented Ca/K record displays a ratio between authigenic carbonate precipitation and siliciclastic
 205 material input from the drainage (Kwiecien et al., 2014). According to Kwiecien et al. (2014), the Ca/K
 206 ratio shows higher values ascribed to higher amounts of authigenic carbonate during warmer periods
 207 (interstadials/interglacial) and lower values related to increasing detrital input during stadials/glacial (Fig.
 208 3C).

209 **5. Discussion**

210 **5.1 Long-term vegetation dynamics at Lake Van**

211 Variations in the orbital configuration of the Earth are responsible for changes in the climate system from
 212 one state to another; on millennial timescales, for glacial-interglacial cycles (Berger, 1978; Berger et al.,
 213 2007). However, higher frequency oscillations (e.g., Dansgaard-Oeschger events; Dansgaard et al., 1993)
 214 are superimposed on the long-term orbitally-driven climate dynamics. These abrupt changes of the climate
 215 system are not directly driven by orbital forcing, but can be interpreted as transitions between two states of
 216 the inter-hemispheric Atlantic Ocean circulation driven by large-scale thermal and salinity gradients (e.g.,
 217 Bond and Lotti, 1995; Cacho et al., 2000, 1999; Chapman and Shackleton, 1999; Hemming, 2004; Hodell
 218 et al., 2008; McManus et al., 1999; Rasmussen et al., 2014; Wolff et al., 2010). In particular, changes in
 219 the oceanic circulation affected regional and local atmospheric circulation patterns, for example, the
 220 strength and position of the westerlies in the Northern Hemisphere, which are responsible for the moisture
 221 supply in eastern Anatolia (Akçar and Schlüchter, 2005, Roberts et al., 2008).

222 According to Jessen and Milthers (1928) and Litt et al. (2014), an interstadial stage is an interval of
 223 temporary improved climate within a glacial phase, which has been either too short to permit full
 224 expansion of thermophilous trees and/or too cold or dry to reach the climate optimum of an interglacial
 225 period in the same region. In comparison, stadial stages correspond to cold/dry intervals marked not only
 226 by global but also by local ice re-advances (Lowe and Walker, 1984).

227 Below, we will discuss only the most pronounced interstadials (e.g., MIS 5c and 5a) and Dansgaard-
 228 Oeschger interstadials (AP >10%; e.g., DO 19, 17-16, 14, 12, 8 and 1), here identified on the basis of the
 229 Lake Van pollen record (see also Litt et al., 2014). All other 'warm/wet' phases with lower expansion of
 230 temperate trees (AP <10%) are not explicitly mentioned in the following section.

231 **5.1.1 MIS 5e-5a**

232 The last interglacial at Lake Van (MIS 5e; 131.2-111.5 ka BP; Pickarski et al., 2015) is characterized by
233 an oak steppe-forest during the climate optimum (129.1-124.1 ka BP), while coniferous species (e.g.,
234 *Pinus*) dominated the late interglacial period between 124.1 and 111.5 ka BP at the minimum peak in
235 summer insolation (Pickarski et al., 2015; Fig. 3A, E). The expansion of dry-tolerant and/or cold-adapted
236 *Pinus* (probably *Pinus nigra*) going along with a reduction of warm-temperate species (e.g., deciduous
237 oak) demonstrates cooler temperatures and summer-dry conditions during the late interglacial period
238 (Pickarski et al., 2015). In this regard, Litt et al. (2014) argued that positive summer temperature
239 anomalies and negative winter temperature anomalies during the late interglacial lead to a strong
240 continentality, more precisely, to strong temperature variations with still low moisture availability in
241 eastern Anatolia.

242 MIS 5d is marked by a significant expansion of steppic herbaceous plants at the expense of wooded
243 landscape, which signals a considerable climate deterioration from ~111.5 to 107.8 ka BP (Herning
244 stadial; AP <20%; Fig. 3E). The regional climate at Lake Van was characterized by a strong seasonal
245 moisture deficiency ($\delta^{18}\text{O}_{\text{bulk}}$ values >2‰, Fig. 3B). The cold/dry climatic conditions with marked
246 seasonality in precipitation during the stadial were responsible for poor soil development and enhanced
247 erosion of regional material as recorded by the Ca/K ratio (Fig. 3C).

248 An abrupt shift in most proxies (pollen data, $\delta^{18}\text{O}_{\text{bulk}}$, Ca/K ratio) displays the onset of two pronounced
249 interstadials at 107.8-87.2 ka BP (Brørup interstadial; MIS 5c) and at 84.9-77.5 ka BP (Odderade
250 interstadial; MIS 5a; Fig. 3). The rapid decrease in steppic herbaceous elements (e.g., Chenopodiaceae)
251 and the slow increase of summer-green oaks suggest that climate in eastern Anatolia became progressively
252 warmer and wetter during these interstadials. Similar to the late interglacial stage (124.1-111.5 ka BP), the
253 Brørup interstadial recorded a slight climatic amelioration that continued with the predominance of cold-
254 and/or summer-dry adapted conifers (*Pinus* >60%, Fig. 3E; *Pinus* concentration >20,000 grains cm⁻³, Fig.
255 2). Changes in seasonal rainfall inferred from depleted $\delta^{18}\text{O}_{\text{bulk}}$ values (up to -2‰) to more positive
256 oxygen isotope signatures (>1‰) and generally lower winter temperatures have a decisive negative impact
257 on moisture-requiring thermophilous plants such as deciduous oaks (<10%, Table 1; Fig. 3E). Therefore,
258 the likely occurrence of deciduous *Quercus* in higher altitudes, for instance at southern slopes of the Bitlis
259 Massif, would be caused by increasing orography-related precipitation amounts (Litt et al., 2014). An
260 open oak steppe-forest, which was predominant during the MIS 5e at Lake Van, did not become dominant
261 at any time during the last glacial (Fig. 3E; Pickarski et al., 2015).

262 The new high-resolution microscopic charcoal data show that fire frequency had an immediate response to
263 climate variability (Fig. 3D). According to previous high-resolution pollen studies by Wick et al. (2003)
264 and Pickarski et al. (2015), rising global temperature and increased moisture availability leads to higher
265 vegetation productivity (e.g., higher vegetation density due to spread of warm-temperate grasslands) that
266 correlates to considerably more fuel for burning during interstadials (>1,000 charcoal particles cm⁻³; Fig.

267 3D). During stadials, lower microscopic charcoal concentrations (between 300 and 850 particles cm^{-3})
 268 characterizes an open dry desert steppe landscape with low vegetation density (e.g., MIS 5b; Daniau et al.,
 269 2010; Sadori et al., 2015; Vanniere et al., 2011; Fig. 3D).

270 After a short-term climatic deterioration between ~87.3 to 84.9 ka BP (MIS 5b; Rederstall stadial, AP
 271 <10%) characterized by a similar expansion of steppic herbaceous plants as documented for MIS 5d
 272 (Herning stadial), the spread of deciduous oaks defined the beginning of the MIS 5a. Environmental
 273 conditions of the Odderade interstadial (MIS 5a; ~85-77 ka BP) are difficult to resolve due to the eruption
 274 of the Incekaya-Dibekli volcano at ~80 ka BP (Sumita and Schmincke, 2013). The fragmentary
 275 documentation of the vegetation signal, primarily due to the respective admixture of pyroclastic material
 276 (Stockhecke et al., 2014b), complicates the study of vegetation and climate evolution at Lake Van.
 277 Nevertheless, the briefly rising AP level (AP >10%) consisting of deciduous *Quercus*, *Betula* and the
 278 sporadic occurrence of *Pistacia* cf. *atlantica*, points to short-term favorable climatic conditions and an
 279 increased moisture availability at the beginning of MIS 5a (Fig. 2, 3E). Relatively high fire intensity
 280 (charcoal concentration up to 2,000 particles cm^{-3} ; Fig. 3D) and lower detrital input (Fig. 3C) support an
 281 advancing vegetation cover due to warmer climatic conditions. However, *Pinus*, which was dominant
 282 during MIS 5c and MIS 5e, is no longer growing in the vicinity of the lake (less than 4%; *Pinus*
 283 concentration <200 grains cm^{-3} , Fig. 2, 3E). The shift from depleted oxygen isotope signature (-1.90‰) to
 284 more positive values (1.81‰, Fig. 3B) confirms the reduction in precipitation and/or increasing
 285 evaporation throughout the MIS 5a.

286 5.2 Abrupt climate changes during MIS 4-2

287 The general dominance of *Artemisia*, Chenopodiaceae, Poaceae and the decrease of arboreal pollen (AP
 288 <10%; mainly deciduous *Quercus* and *Pinus*) in the glacial pollen spectra indicate a wide spread of arid
 289 desert steppe vegetation in eastern Anatolia between ~75-12 ka BP (Fig. 2, 3). However, the total absence
 290 of moisture-requiring thermophilous arboreal species such as *Ulmus* and *Carpinus betulus* or frost-
 291 sensitive taxa (e.g., *Pistacia* cf. *atlantica*, evergreen *Quercus*), a low vegetation density, a high terrigenous
 292 input (of fluvial and/or eolian origin; Fig. 3C), a consistently positive $\delta^{18}\text{O}_{\text{bulk}}$ signature (~0.77‰; Fig.
 293 3B), and a decreasing microscopic charcoal concentration (from ~1,700 to <400 particles cm^{-3} ; Fig. 3D)
 294 point to a strong aridification and cooling in eastern Anatolia after 70 ka BP. The observation is consistent
 295 with low summer insolation (Berger, 1978; Berger et al., 2007), increased global ice volume (Shackleton,
 296 1987), and cooler sea surface temperature (SST; Cacho et al., 2000), which, combined with the
 297 atmospheric effects of a weakening AMOC (Atlantic Meridional Overturning Circulation; Böhm et al.,
 298 2015; Bond et al., 1993) contributed to a widespread aridity across the Mediterranean region (e.g.,
 299 Fletcher et al., 2010; Kwiecien et al., 2009; Sánchez Goñi et al., 2002).

300 During MIS 4 to 2, high-frequency vegetation and environmental oscillations in the Lake Van proxies
 301 demonstrate a reproducible pattern of centennial to millennial-scale alternation between DO interstadials
 302 and DO stadials (Fig. 4; Dansgaard et al., 1993; NGRIP members, 2004; Rasmussen et al., 2014; Sánchez
 303 Goñi and Harrison, 2010; Svensson et al., 2006; Wolff et al., 2010). In comparison with the Greenland
 304 isotope curve, intervals with lighter $\delta^{18}\text{O}$ NGRIP values (DO stadials) coincide with lower percentages of
 305 AP (Fig. 3E). An increase in deciduous *Quercus* percentages, which is an important criterion for initial
 306 warming intervals during Termination 1 (Litt et al., 2014; 2009; Wick et al., 2003) and Termination 2
 307 (Pickarski et al., 2015), is characteristic for each DO interstadial (Fig. 3E).

308 In general, the abrupt variability of temperate AP from Lake Van and $\delta^{18}\text{O}$ NGRIP values are more or less
 309 synchronous (Fig. 4). Leads and lags between the proxy records, illustrated in detail in Fig. 5, are difficult
 310 to assess due to their heterogeneous resolution. In any case, we cannot expect a perfect matching between
 311 biotic and abiotic proxies related to climate events due to their different response time. In addition, the
 312 lack of correspondence between the pollen signal and the timing of some DO events could also be
 313 explained by uncertainties in the current age-depth model. Still, as expected from various eastern
 314 Mediterranean pollen records, the Lake Van pollen record documents that temperate taxa tend to reach
 315 their maxima after the onset of a warming phase and, therefore, lag behind the Ca/K increase, which
 316 responds immediately to climate changes (Fig. 5).

317 The longest and most pronounced variability of tree populations in the Lake Van pollen record is shown
 318 during the MIS 3 (~60-28 ka BP; PAZ IIa3-2) suggesting a rapid alternation of warmer/wetter interstadials
 319 and cooler/drier stadials. High-amplitude variations in the Ca/K ratio of Lake Van sediments indicate
 320 changes in erosion of regional material, due to unstable environmental condition in the catchment area.
 321 Larger interstadials such as DO 19, 17-16, 14, 12, and 8 are indicated by peaks in the Ca/K ratio, which
 322 are concurrent with AP maxima and increased regional fire frequency (Fig. 5). As described above, this
 323 millennial-scale variability in the proxy record was indirectly modulated by orbital-driven changes and
 324 variations in the atmospheric circulation of the Northern Hemisphere (e.g., Cacho et al., 2000, 1999;
 325 Chapman and Shackleton, 1999; Hemming, 2004; Hodell et al., 2008; McManus et al., 1999; Rasmussen
 326 et al., 2014, Wolff et al., 2010). Consequently, the vegetation and environmental conditions at Lake Van
 327 responds to abrupt shifts in temperature and moisture availability related to the position and strength of the
 328 westerlies, which brought mild and humid conditions from the North Atlantic into the eastern
 329 Mediterranean region (Akçar and Schlüchter, 2005, Allen et al., 1999; Fletcher et al., 2010; Müller et al.,
 330 2011; Roberts et al., 2008). The Lake Van $\delta^{18}\text{O}_{\text{bulk}}$ signature supports the suggestion of favorable
 331 environment by the receipt of isotopically depleted meltwater supply and/or increased precipitation
 332 between ~57 and 54 ka BP ($\delta^{18}\text{O}_{\text{bulk}}$ from -1.21 up to ~1‰; Fig. 3B). Furthermore, we propose that the
 333 interval of constantly heavier $\delta^{18}\text{O}_{\text{bulk}}$ values during DO 14 to 12 reflect higher evaporation at Lake Van.

334 The most pronounced DO stadials, i.e. the stadials preceding DO 17, 12, 8, 4, and DO 1 refer to Heinrich
 335 events (HE) 6, HE 5, HE 4, HE 3, and HE 1 (Fig., 4A; Bond and Lotti, 1995; Bond et al., 1993; Heinrich,
 336 1988). The reduction of oceanic heat transport (weakening or shut down of the AMOC; Böhm et al., 2014;
 337 Bond and Lotti, 1995; Bond et al., 1993; Broecker, 1994; Cacho et al., 2000, 1999; Chapman and
 338 Shackleton, 1999) led to significantly cooler Mediterranean SST's and climatic conditions in the
 339 Mediterranean region (e.g., Allen et al., 1999; Fletcher et al., 2010; Müller et al., 2011; Sánchez Goñi et
 340 al., 2002; Tzedakis, 2005; Tzedakis et al., 2004). According to Kwiecien et al. (2009), a decreasing
 341 atmosphere-sea surface thermal gradient of the Mediterranean Sea would have caused a reduction in the
 342 frequency and strength of storm tracks, which were responsible for an intensifying aridity in the Eastern
 343 Mediterranean region. However, since tree populations were already limited at Lake Van during the last
 344 glacial (<10% AP), the pollen signal is relatively insensitive to severe climatic deterioration such as
 345 Heinrich events. Hence, both types of stadials, Heinrich events and DO stadials, lead to a similar reduction
 346 of tree taxa (mainly deciduous *Quercus*), and therefore cannot be clearly distinguished from an average
 347 cooling event (Fig. 4B). An exception might be the HE 5 (~49 ka BP; Fig. 4A). A collapse of AP taxa
 348 from 10% to less than 2% (Fig. 4B) and a short-term detrital supply (Fig. 3C) show that the climate of HE
 349 5 was as cold/dry as the glacial maximum of MIS 4 between 70 and 60 ka BP.

350 Between ~28 and 14 ka BP (PAZ IIa2), very low AP percentages (<10%; Fig. 3E) and a decreasing fire
 351 frequency (Fig. 3D) without significant fluctuations underline considerably stable climate conditions but
 352 pronounced regional cooling and aridity in comparison to MIS 3. It led to an overall reduction in
 353 terrestrial biomass production and thus to a decrease in fuel availability for burning in the catchment area.
 354 Furthermore, the presence of *Juniperus*, indicative for an unstable soil cover, enhanced minerogenic input
 355 into the lake (low Ca/K; Fig. 3C) and a drop in $\delta^{18}\text{O}_{\text{bulk}}$ values (up to -1.6‰; Fig. 3B) support the
 356 assumption of wide open plains around Lake Van. Insolation changes became the major driver (e.g., low
 357 summer insolation, Fig. 3A) and leads to a cooling of global climatic conditions, which results in a
 358 maximum ice extent of the Northern Hemisphere during the last glacial maximum (LGM; Cacho et al,
 359 2000, 1999; Chapman and Shackleton, 1999; NGRIP members, 2004; Rasmussen et al., 2014; Sánchez
 360 Goñi and Harrison, 2010; Wolff et al., 2010).

361 After the LGM (at 21 ± 2 ka; Tzedakis, 2007 and references therein), high summer insolation (Fig. 3A),
 362 decreasing global ice volume (Wolff et al., 2010), the resumption of the westerly activity, enhanced
 363 precipitation (depleted $\delta^{18}\text{O}_{\text{bulk}}$ values; Fig. 3B), and locally rising temperatures in eastern Anatolia
 364 promoted an expansion of an oak steppe-forest at Lake Van (DO 1 at ~14 ka BP; synonymous with the
 365 Bølling-Allerød warm period; Fig. 3E, 4). However, the Late Glacial-Holocene transition (Termination I)
 366 was interrupted by the impact of the Younger Dryas (YD) climate reversal between ~12.8 to 11.6 ka BP
 367 (Litt et al., 2009; Wick et al., 2003). This dramatic event is characterized by the $\delta^{18}\text{O}_{\text{bulk}}$ peak (4.46 ‰;
 368 Fig. 3B), by the drop of the charcoal concentration (<1,000 particles cm^{-3} ; Fig. 3D), and by the rapid

369 increase of arid desert steppe plants (up to 70%; Fig. 2B). Further details about the Late Glacial and early
 370 Holocene pollen and microscopic charcoal record of Lake Van are not considered here, as Litt et al.
 371 (2009) and Wick et al. (2003) already presented vegetation and inferred environmental conditions for that
 372 period.

373 **5.3 Comparison with palynological records from the Mediterranean and Black Sea region**

374 A regional comparison between Lake Van and pollen archives from the central (Lago Grande di
 375 Monticchio, Italy; Allen et al., 1999) and the eastern Mediterranean regions (Tenaghi Philippon, Greece;
 376 Müller et al., 2011), the south eastern Levantine Basin (Core 9509; Langgut et al., 2011), and the Black
 377 Sea (Shumilovskikh et al., 2014, 2012) is presented in Fig. 4. Despite differences in elevation, topography
 378 and chronology, the palaeoenvironmental investigation indicates a good match based on the similar main
 379 trends of the major vegetation elements between the five pollen records. It should be noted that the
 380 Monticchio sequence features an independent chronology based on varve counting. Climatic
 381 teleconnections between the North Atlantic, Black Sea and different parts of the Mediterranean region are
 382 expressed by coeval minima in AP during stadials, suggesting cold and dry conditions and a rather open
 383 landscape, in particular in MIS 4 and MIS 2. Between 60 and 45 ka BP, the pollen record from Lake Van
 384 reveals a period of increased tree vegetation, which are interpreted as the signature of enhanced
 385 precipitation and higher temperature (DO 17-12; Fig. 4B, grey bars). According to Müller et al. (2011),
 386 this period was described as the North African Humid Period (NAHP; ca. 55-49 ka BP), where the
 387 anatomically modern humans (AMH) migrate from Africa via the Levant to Europe. During that time,
 388 climatic conditions in the eastern Mediterranean were more humid and milder as indicated by an abrupt
 389 shift from desert-steppe vegetation to semi-arid grassland at Lake Van (AP ~10%; Fig. 4B) and to open
 390 forest vegetation (AP up to 70%, Fig. 4E) in the Tenaghi Philippon area (Müller et al., 2011). The marine
 391 pollen record from the south eastern Levantine basin (Fig. 4C) also points to increasing AP percentages
 392 during ~56.0 and 44.5 ka BP (Langgut et al., 2011).

393 However, there are some differences between the pollen records. More developed forests exist around the
 394 central and eastern Mediterranean Sea and the Black Sea compared to the Near East. Despite the intensive
 395 aridification in eastern Anatolia during glacials, the vegetation composition of Lake Van and the
 396 Levantine Basin differs from the terrestrial Mediterranean pollen records. Firstly, drought-sensitive taxa
 397 such as *Ulmus*, *Carpinus betulus* and *Fagus* were frequently present in Italy, e.g., at Lago Grande di
 398 Monticchio, Valle di Castiglione, Stracciacappa and Lagaccione (Allen et al., 1999; Follieri et al., 1998)
 399 even during stadials. Secondly, the high-resolution Tenaghi Philippon and Ioannina sequences (Müller et
 400 al., 2011; Tzedakis et al., 2002) show that thermophilous trees (deciduous *Quercus*) increased rapidly
 401 during each interstadial without migrational lags (Fig. 4G, F). It suggests that these sites were better suited
 402 in sustaining refugial temperate tree population due to the effects of orographic precipitation. Thirdly,

403 both the diversity and the low amplitude of variations in temperate tree taxa (e.g., deciduous *Quercus*) of
 404 the eastern Mediterranean pollen records (Lake Van and Levantine Basin; Fig. 4C) indicates greater
 405 distances and/or slow migration rates from refugia during the glacial interval. Such areas might be found
 406 in the south and south-east Black Sea Mountains (Euxinian vegetation) and the Caucasus mountains
 407 (Hyrcanian vegetation), which receive increased atmospheric moisture and higher orographic precipitation
 408 from the Black Sea (Bottema, 1986; Leroy and Arpe, 2007; Shumilovskikh et al., 2012). Especially the
 409 Black Sea region was characterized by mean winter temperatures close to or above 0°C during the last
 410 glacial (Shumilovskikh et al., 2014).

411 Moreover, the different vegetation development in the Mediterranean region demonstrates a W-E
 412 vegetation gradient from an open temperate forest (including evergreen species) in the central (Allen et al.,
 413 1999; Follieri et al., 1998) and eastern Mediterranean (Müller et al., 2011) to a semi-arid grassland in the
 414 Near East, where the availability of precipitation is the limiting factor for the establishment of an open oak
 415 steppe-forest. This moisture gradient reflects an increasing continental affect and a decreasing influence of
 416 changes in the atmospheric circulation of the Northern Hemisphere.

417 6. Conclusions

- 418 1. By using a range of paleoenvironmental proxies, we were able to detect subtle climate changes
 419 even during generally cold and arid glacial phases. This study illustrates the great potential of
 420 Lake Van as an archive of Eastern Mediterranean climate and environment over the entire
 421 Quaternary.
- 422 2. Our new palynological results show the climatic teleconnection between Lake Van and the
 423 Atlantic Ocean. It reflects the complex underlying drivers of high frequency regional climate and
 424 environmental variability caused by seasonal insolation changes, ice sheet dynamics, and the
 425 ocean circulation in the North Atlantic.
- 426 3. The comparison with central and eastern Mediterranean and Black Sea pollen sequences reveals a
 427 W-E gradient of decreasing moisture in the Mediterranean region due to an increasing continental
 428 effect and a reduction of the atmospheric impact of the North Atlantic Ocean.
- 429 4. Dansgaard-Oeschger cycles are clearly recognized in the Lake Van pollen record and by other
 430 abiotic proxies. Interstadials are characterized by the spread of temperate vegetation (e.g.,
 431 deciduous *Quercus*) suggesting regional moisture availability. Stadials can be recognized by the
 432 dominance of steppe elements (e.g., *Artemisia*, *Chenopodiaceae*) pointing to cold temperature and
 433 an increasing aridity.
- 434 5. Heinrich events cannot clearly be distinguished from an average cooling event (stadials). They
 435 show a similar impact on the vegetation and the environment.

436 6. The supply of detrital material seems to respond directly to changes in the vegetation composition,
 437 e.g., the terrestrial supply is low (high authigenic carbonate precipitation) when the vegetation
 438 cover in the catchment area is dense. In contrast, an open landscape favors a physical erosion
 439 including local detrital and dust input.

440 7. Moreover, the fire frequency at Lake Van indicates an immediate link to climate changes. The fire
 441 frequency is high when global temperatures and regional moisture levels increase providing a
 442 higher terrestrial biomass production.

443 **Data availability**

444 The complete pollen dataset is available on the PANGAEA database
 445 (<http://doi.pangaea.de/10.1594/PANGAEA.853814>), and the microscopic charcoal record can be found on
 446 the Global Charcoal Database (GCD; www.paleofire.org).

447 **Acknowledgements**

448 This study is a contribution to the Lake Van Drilling Project PALEOVAN funded by the International
 449 Continental Scientific Drilling Program (ICDP), the Swiss National Science Foundation (SNF) and the
 450 Scientific and Technological Research Council of Turkey (Tübitak). Financial support was provided by
 451 the German Research Foundation (DFG; LI 582/15-1-2). We thank the scientific PALEOVAN team for
 452 their support during the sampling campaign, and for sharing data. We kindly thank Ulla Röhl, Alex
 453 Wübers and Hans-Joachim Wallrabe-Adams from the IODP Core Repository in Bremen (MARUM) for
 454 their help during the sampling campaign. We thank Dr. Nils Andersen and his working team at the
 455 Leibnitz-Laboratory for Radiometric Dating and Isotope Research for the measurements of the oxygen
 456 isotope samples. N. Pickarski thanks Karen Schmeling and Beate Söntgerath for the pollen preparation,
 457 Manuela Rüßmann and Hannah Vossel for their support in the lab, and all colleagues from the Department
 458 of Palaobotany. The authors are grateful to Dominik Fleitmann for editing of the manuscript. Laura Sadori
 459 and an anonymous reviewer are acknowledged for their constructive comments and useful
 460 recommendations, which improved the quality of this manuscript.

461 **References**

462 Akçar, N., Schlüchter, C., 2005. Paleoglaciations in Anatolia: A Schematic Review and First Results.
 463 *Eiszeitalter und Gegenwart* 55, 102–121.

464 Allen, J.R., Brandt, U., Brauer, A., Hubberten, H.-W., Huntley, B., Keller, J., Kraml, M., Mackensen, A.,
 465 Mingram, J., Negendank, J.F., 1999. Rapid environmental changes in southern Europe during the
 466 last glacial period. *Nature* 400, 740–743. doi:10.1038/23432

467 Allen, J.R.M., Watts, W.A., Huntley, B., 2000. Weichselian palynostratigraphy, palaeovegetation and
 468 palaeoenvironment; the record from Lago Grande di Monticchio, southern Italy. *EDLP - Med*
 469 *Special* 73-74, 91–110. doi:10.1016/S1040-6182(00)00067-7

470 Alvarez-Solas, J., Ramstein, G., 2011. On the triggering mechanism of Heinrich events. *Proceedings of*
 471 *the National Academy of Sciences* 108, E1359–E1360. doi:10.1073/pnas.1116575108

472 Berger, A., 1978. Long-term variations of daily insolation and Quaternary climate changes. *Journal of*
 473 *Atmospheric Sciences* 35, 2362–2367. doi:[http://dx.doi.org/10.1175/1520-0469\(1978\)035<2362:LTVIDI>2.0.CO;2](http://dx.doi.org/10.1175/1520-0469(1978)035<2362:LTVIDI>2.0.CO;2)

474 Berger, A., Loute, M.F., Kaspar, F., Lorenz, S.J., 2007. Insolation During Interglacial, in: Sirocko, F.,
 475 Claussen, M., Sánchez Goñi, M.F., Litt, T. (Eds.), *The Climate of Past Interglacial*. Elsevier,
 476 Amsterdam, pp. 13–27.

477 Berglund, B.E., Ralska-Jasiewiczowa, M., 1986. Pollen anaylsis and pollen diagrams, in: Berglund, B.E.,
 478 Ralska-Jasiewiczowa, M. (Eds.), *Handbook of Holocene Palaeoecology and Palaeohydrology*.
 479 John Wiley and Sons, pp. 455–484.

480 Beug, H.-J., 2004. *Leitfaden der Pollenbestimmung für Mitteleuropa und angrenzende Gebiete*. Pfeil,
 481 München.

482 Blunier, T., Brook, E.J., 2001. Timing of Millennial-Scale Climate Change in Antarctica and Greenland
 483 During the Last Glacial Period. *Science* 291, 109–112. doi:10.1126/science.291.5501.109

484 Böhm, E., Lippold, J., Gutjahr, M., Frank, M., Blaser, P., Antz, B., Fohlmeister, J., Frank, N., Andersen,
 485 M.B., Deininger, M., 2015. Strong and deep Atlantic meridional overturning circulation during
 486 the last glacial cycle. *Nature* 517, 73–76. doi:10.1038/nature14059

487 Bond, G.C., Broecker, W.S., Johnsen, S., McManus, J., Labeyrie, L., Jouzel, J., Bonani, G., 1993.
 488 Correlations between climate records from North Atlantic sediments and Greenland ice. *Nature*
 489 365, 143–147. doi:10.1038/365143a0

490 Bond, G.C., Heinrich, H., Broecker, W.S., Labeyrie, L., McManus, J., Andrews, J., Huon, S., Jantschik,
 491 R., Clasen, S., Simet, C., Tedesco, K., Klas, M., Bonani, G., Ivy, S., 1992. Evidence for massive
 492 discharges of icebergs into the North Atlantic ocean during the last glacial period. *Nature* 360,
 493 245–249.

494 Bond, G.C., Lotti, R., 1995. Iceberg Discharges into the North Atlantic on Millennial Time Scales During
 495 the Last Glaciation. *Science* 267, 1005–1010. doi:10.1126/science.267.5200.1005

496 Bottema, S., 1986. A late quaternary pollen diagram from Lake Urmia (Northwestern Iran). *Review of*
 497 *Palaeobotany and Palynology* 47, 241–261. doi:10.1016/0034-6667(86)90039-4

498 Broecker, W.S., 1994. Massive iceberg discharges as triggers for global climate change. *Nature* 372, 421–
 499 424. doi:10.1038/372421a0 Cacho, I., Grimalt, J.O., Pelejero, C., Canals, M., Sierro, F.J., Flores,
 500 J.A., Shackleton, N., 1999. Dansgaard-Oeschger and Heinrich event imprints in Alboran Sea
 501 paleotemperatures. *Paleoceanography* 14, 698–705. doi:10.1029/1999PA900044

502 Cacho, I., Grimalt, J.O., Sierro, F.J., Shackleton, N.J. s, Canals, M., 2000. Evidence for enhanced
 503 Mediterranean thermohaline circulation during rapid climatic coolings. *Earth and Planetary
 504 Science Letters* 183, 417–429. doi:10.1016/S0012-821X(00)00296-X

505 Chapman, M.R., Shackleton, N.J., 1999. Global ice-volume fluctuations, North Atlantic ice-rafting events,
 506 and deep-ocean circulation changes between 130 and 70 ka. *Geology* 27, 795–798.
 507 doi:10.1130/0091-7613(1999)027<0795:GIVFNA>2.3.CO;2

508 Clark, J.S., Lynch, J., Stocks, B.J., Goldammer, J.G., 1998. Relationships between charcoal particles in air
 509 and sediments in west-central Siberia. *The Holocene* 8, 19–29.
 510 doi:10.1191/095968398672501165 Daniau, A.-L., Harrison, S.P., Bartlein, P.J., 2010. Fire regimes
 511 during the Last Glacial. *Quaternary Science Reviews* 29, 2918–2930.
 512 doi:10.1016/j.quascirev.2009.11.008

513 Dansgaard, W., Johnsen, S.J., Clausen, H.B., Dahl-Jensen, D., Gundestrup, N.S., Hammer, C.U.,
 514 Hvidberg, C.S., Steffensen, J.P., Sveinbjörnsdóttir, A.E., Jouzel, J., Bond, G., 1993. Evidence for
 515 general instability of past climate from a 250-kyr ice-core record. *Nature* 364, 218–220.

516 Degens, E.T., Kurtman, F., 1978. The Geology of Lake Van. *The Mineral Research and Exploration
 517 Institute of Turkey*, Ankara.

518 Faegri, K., Iversen, J., 1993. *Bestimmungsschlüssel für die nordwesteuropäische Pollenflora*. Gustav
 519 Fischer, Jena.

520 Fletcher, W.J., Sánchez Goñi, M.F., Allen, J.R.M., Cheddadi, R., Combourieu-Nebout, N., Huntley, B.,
 521 Lawson, I., Londeix, L., Magri, D., Margari, V., Müller, U.C., Naughton, F., Novenko, E.,
 522

523 Roucoux, K., Tzedakis, P.C., 2010. Millennial-scale variability during the last glacial in
 524 vegetation records from Europe. *Vegetation Response to Millennial-scale Variability during the*
 525 *Last Glacial* 29, 2839–2864. doi:10.1016/j.quascirev.2009.11.015

526 Follieri, M., Giardini, M., Magri, D., Sadori, L., 1998. PALYNOSTRATIGRAPHY OF THE LAST
 527 GLACIAL PERIOD IN THE VOLCANIC REGION OF CENTRAL ITALY. *Quaternary*
 528 *International* 47–48, 3–20. doi:10.1016/S1040-6182(97)00065-7

529 Frey, W., Kürschner, H., 1989. Die Vegetation im Vorderer Orient. *Erläuterungen zur Karte A VI 1*
 530 *Vorderer Orient. Vegetation des "Tübinger Atlas des Vorderen Orients"., Reihe A. Tübinger Atlas*
 531 *des Vorderen Orients*, Wiesbaden.

532 Heinrich, H., 1988. Origin and consequences of cyclic ice rafting in the Northeast Atlantic Ocean during
 533 the past 130,000 years. *Quaternary Research* 29, 142–152. doi:10.1016/0033-5894(88)90057-9

534 Hemming, S.R., 2004. Heinrich events: Massive late Pleistocene detritus layers of the North Atlantic and
 535 their global climate imprint. *Reviews of Geophysics* 42, RG1005. doi:10.1029/2003RG000128

536 Hodell, D.A., Channell, J.E.T., Curtis, J.H., Romero, O.E., Röhl, U., 2008. Onset of "Hudson Strait"
 537 Heinrich events in the eastern North Atlantic at the end of the middle Pleistocene transition (~640
 538 ka)? *Paleoceanography* 23, PA4218. doi:10.1029/2008PA001591

539 Jessen, A., Milthers, V., 1928. Stratigraphical and paleontological studies of interglacial freshwater
 540 deposits in Jutland and Northwest Germany. *Danmarks Geologiske Undersøgelse* 48, 1–379.

541 Kwiecien, O., Arz, H.W., Lamy, F., Plessen, B., Bahr, A., Haug, G.H., 2009. North Atlantic control on
 542 precipitation pattern in the eastern Mediterranean/Black Sea region during the last glacial.
 543 *Quaternary Research* 71, 375–384. doi:10.1016/j.yqres.2008.12.004

544 Kwiecien, O., Stockhecke, M., Pickarski, N., Heumann, G., Litt, T., Sturm, M., Anselmetti, F., Kipfer, R.,
 545 Haug, G.H., 2014. Dynamics of the last four glacial terminations recorded in Lake Van, Turkey.
 546 *Quaternary Science Reviews* 104, 42–52. doi:10.1016/j.quascirev.2014.07.001

547 Langgut, D., Almogi-Labin, A., Bar-Matthews, M., Weinstein-Evron, M., 2011. Vegetation and climate
 548 changes in the South Eastern Mediterranean during the Last Glacial-Interglacial cycle (86 ka):
 549 new marine pollen record. *Quaternary Science Reviews* 30, 3960–3972.
 550 doi:10.1016/j.quascirev.2011.10.016

551 Lemcke, G., Sturm, M., 1997. $\delta^{18}\text{O}$ and Trace Element Measurements as Proxy for the Reconstruction of
 552 Climate Changes at Lake Van (Turkey): Preliminary Results, in: Dalfes, H.N., Kukla, G., Weiss,
 553 H. (Eds.), *Third Millennium BC Climate Change and Old World Collapse*, NATO ASI Series.
 554 Springer Berlin Heidelberg, pp. 653–678.

555 Leroy, S.A.G., Arpe, K., 2007. Glacial refugia for summer-green trees in Europe and south-west Asia as
 556 proposed by ECHAM3 time-slice atmospheric model simulations. *Journal of Biogeography* 34,
 557 2115–2128. doi:10.1111/j.1365-2699.2007.01754.x

558 Lézine, A.-M., von Grafenstein, U., Andersen, N., Belmecheri, S., Bordon, A., Caron, B., Cazet, J.-P.,
 559 Erlenkeuser, H., Fouache, E., Grenier, C., Huntsman-Mapila, P., Hureau-Mazaudier, D., Manelli,
 560 D., Mazaud, A., Robert, C., Sulpizio, R., Tiercelin, J.-J., Zanchetta, G., Zeqollari, Z., 2010. Lake
 561 Ohrid, Albania, provides an exceptional multi-proxy record of environmental changes during the
 562 last glacial-interglacial cycle. *Palaeogeography, Palaeoclimatology, Palaeoecology* 287, 116–127.
 563 doi:10.1016/j.palaeo.2010.01.016

564 Litt, T., Anselmetti, F.S., 2014. Lake Van deep drilling project PALEOVAN. *Quaternary Science*
 565 *Reviews* 104, 1–7. doi:10.1016/j.quascirev.2014.09.026

566 Litt, T., Anselmetti, F.S., Baumgarten, H., Beer, J., Çagatay, N., Cukur, D., Damci, E., Glombitza, C.,
 567 Haug, G., Heumann, G., Kallmeyer, J., Kipfer, R., Krastel, S., Kwiecien, O., Meydan, A.F.,
 568 Orcen, S., Pickarski, N., Randlett, M.-E., Schmincke, H.-U., Schubert, C.J., Sturm, M., Sumita,
 569 M., Stockhecke, M., Tomonaga, Y., Vigliotti, L., Wonik, T., team, the P. scientific, 2012.
 570 500,000 Years of Environmental History in Eastern Anatolia: The PALEOVAN Drilling Project.
 571 *Scientific Drilling Journal* 18–29. doi:10.5194/sd-14-18-2012

572 Litt, T., Krastel, S., Sturm, M., Kipfer, R., Örcen, S., Heumann, G., Franz, S.O., Ülgen, U.B., Niessen, F.,
 573 2009. "PALEOVAN", International Continental Scientific Drilling Program (ICDP): site survey
 574 results and perspectives. *Quaternary Science Reviews* 28, 1555–1567.
 575 doi:10.1016/j.quascirev.2009.03.002

576 Litt, T., Pickarski, N., Heumann, G., Stockhecke, M., Tzedakis, P.C., 2014. A 600,000 year long
 577 continental pollen record from Lake Van, eastern Anatolia (Turkey). *Quaternary Science Reviews*
 578 104, 30–41. doi:10.1016/j.quascirev.2014.03.017

579 Lowe, J.J., Walker, M.J.C., 1984. *Reconstructing Quaternary Environments*, 2nd ed. Longman,
 580 Edinburgh.

581 McManus, J.F., Oppo, D.W., Cullen, J.L., 1999. A 0.5-Million-Year Record of Millennial-Scale Climate
 582 Variability in the North Atlantic. *Science* 283, 971–975. doi:10.1126/science.283.5404.971

583 Moore, P.D., Webb, J.A., Collinson, M.E., 1991. *Pollen Analysis*. Blackwell Science.

584 Müller, U.C., Pross, J., Tzedakis, P.C., Gamble, C., Kotthoff, U., Schmiedl, G., Wulf, S., Christianis, K.,
 585 2011. The role of climate in the spread of modern humans into Europe. *Quaternary Science
 586 Reviews* 30, 273–279. doi:10.1016/j.quascirev.2010.11.016

587 NGRIP members, 2004. High-resolution record of Northern Hemisphere climate extending into the last
 588 interglacial period. *Nature* 431, 147–151. doi:10.1038/nature02805

589 Panagiotopoulos, K., Böhm, A., Leng, M., Wagner, B., Schäbitz, F., 2014. Climate variability over the last
 590 92 ka in SW Balkans from analysis of sediments from Lake Prespa. *Climate of the Past* 10, 643–
 591 660. doi:10.5194/cp-10-643-2014

592 Pickarski, N., Kwiecien, O., Djamali, M., Litt, T., 2015. Vegetation and environmental changes during the
 593 last interglacial in eastern Anatolia (Turkey): a new high-resolution pollen record from Lake Van.
 594 *Palaeogeography, Palaeoclimatology, Palaeoecology* 435, 145–158.
 595 <http://dx.doi.org/10.1016/j.palaeo.2015.06.015>

596 Punt, W., 1976. *The Northwest European Pollen Flora*. Elsevier, Amsterdam.

597 Rasmussen, S.O., Andersen, K.K., Svensson, A.M., Steffensen, J.P., Vinther, B.M., Clausen, H.B.,
 598 Siggaard-Andersen, M.-L., Johnsen, S.J., Larsen, L.B., Dahl-Jensen, D., Bigler, M., Röthlisberger,
 599 R., Fischer, H., Goto-Azuma, K., Hansson, M.E., Ruth, U., 2006. A new Greenland ice core
 600 chronology for the last glacial termination. *Journal of Geophysical Research: Atmospheres* 111,
 601 D06102. doi:10.1029/2005JD006079

602 Rasmussen, S.O., Bigler, M., Blockley, S.P., Blunier, T., Buchardt, S.L., Clausen, H.B., Cvijanovic, I.,
 603 Dahl-Jensen, D., Johnsen, S.J., Fischer, H., Gkinis, V., Guillecic, M., Hoek, W.Z., Lowe, J.J.,
 604 Pedro, J.B., Popp, T., Seierstad, I.K., Steffensen, J.P., Svensson, A.M., Vallelonga, P., Vinther,
 605 B.M., Walker, M.J.C., Wheatley, J.J., Winstrup, M., 2014. A stratigraphic framework for abrupt
 606 climatic changes during the Last Glacial period based on three synchronized Greenland ice-core
 607 records: refining and extending the INTIMATE event stratigraphy. *Quaternary Science Reviews*
 608 106, 14–28. doi:10.1016/j.quascirev.2014.09.007

609 Reille, M., 1995. Pollen et Spores d'Europe et d'Afrique du Nord (Supplement 1). Laboratoire de
 610 Botanique Historique et Palynologie, Marseille.

611 Reille, M., 1998. Pollen et Spores d'Europe et d'Afrique du Nord (Supplement 2). Laboratoire de
 612 Botanique Historique et Palynologie, Marseille.

613 Reille, M., 1999. Pollen et Spores d'Europe et d'Afrique du Nord. Laboratoire de Botanique Historique et
 614 Palynologie, Marseille.

615 Roberts, N., Jones, M.D., Benkaddour, A., Eastwood, W.J., Filippi, M.L., Frogley, M.R., Lamb, H.F.,
 616 Leng, M.J., Reed, J.M., Stein, M., Stevens, L., Valero-Garcés, B., Zanchetta, G., 2008. Stable
 617 isotope records of Late Quaternary climate and hydrology from Mediterranean lakes: the
 618 ISOMED synthesis. *Quaternary Science Review* 27, 2426–2441.
 619 <http://dx.doi.org/10.1016/j.quascirev.2008.09.005>

620 Sadoni, L., Masi, A., Ricotta, C. (2015). Climate-driven past fires in central Sicily. *Plant Biosystems* 149,
 621 166–173. doi:10.1080/11263504.2014.992996

622 Sánchez Goñi, M.F., Cacho, I., Turon, J.-L., Guiot, J., Sierro, F.J., Peyrouquet, J.-P., Grimalt, J.O.,
 623 Shackleton, N.J., 2002. Synchronicity between marine and terrestrial responses to millennial scale
 624 climatic variability during the last glacial period in the Mediterranean region. *Climate Dynamics*
 625 19, 95–105. doi:DOI 10.1007/s00382-001-0212-x

626 Sánchez Goñi, M.F., Harrison, S.P., 2010. Introduction: Millennial-scale climate variability and
 627 vegetation changes during the Last Glacial: Concepts and terminology. *Quaternary Science
 628 Reviews* 29, 2823–2827. doi:10.1016/j.quascirev.2009.11.014

629 Shackleton, N.J., 1987. Oxygen isotopes, ice volume and sea level. *Quaternary Science Reviews* 6, 183–
 630 190. doi:10.1016/0277-3791(87)90003-5

631 Shumilovskikh, L.S., Fleitmann, D., Nowaczyk, N.R., Behling, H., Marret, F., Wegwerth, A., Arz, H.W.,
 632 2014. Orbital- and millennial-scale environmental changes between 64 and 20 ka BP recorded in
 633 Black Sea sediments. *Climate of the Past* 10, 939–954. doi:10.5194/cp-10-939-2014

634 Shumilovskikh, L.S., Tarasov, P., Arz, H.W., Fleitmann, D., Marret, F., Nowaczyk, N., Plessen, B.,
 635 Schlütz, F., Behling, H., 2012. Vegetation and environmental dynamics in the southern Black Sea
 636 region since 18 kyr BP derived from the marine core 22-GC3. *Palaeogeography,
 637 Palaeoclimatology, Palaeoecology* 337–338, 177–193.

638 Stockhecke, M., Kwiecien, O., Vigliotti, L., Litt, T., Pickarski, N., Schmincke, H.-U., Çağatay, N., 2014a.
 639 Chronology of the 600 ka old long continental record of Lake Van: climatostratigraphic
 640 synchronization and dating. *Quaternary Sciences Reviews* 104, 8–17.
 641 <http://dx.doi.org/10.1016/j.quascirev.2014.04.008>

642 Stockhecke, M., Sturm, M., Brunner, I., Schmincke, H., Sumita, M., Kipfer, R., Cukur, D., Kwiecien, O.,
 643 Anselmetti, F.S., 2014b. Sedimentary evolution and environmental history of Lake Van (Turkey)
 644 over the past 600 000 years. *Sedimentology* 61, 1830–1861. doi: 10.1111/sed.12118

645 Stockmarr, J., 1971. Tablets with spores used in absolute pollen analysis. *Pollen et Spores* 13, 615–621.

646 Sumita, M., Schmincke, H.-U., 2013. Impact of volcanism on the evolution of Lake Van II: Temporal
 647 evolution of explosive volcanism of Nemrut Volcano (eastern Anatolia) during the past ca. 0.4
 648 Ma. *Journal of Volcanology and Geothermal Research* 253, 15–34.
 649 doi:10.1016/j.jvolgeores.2012.12.009

650 Svensson, A., Andersen, K.K., Bigler, M., Clausen, H.B., Dahl-Jensen, D., Davies, S.M., Johnsen, S.J.,
 651 Muscheler, R., Parrenin, F., Rasmussen, S.O., Röhlisberger, R., Seierstad, I., Steffensen, J.P.,
 652 Vinther, B.M., 2008. A 60 000 year Greenland stratigraphic ice core chronology. *Climate of the
 653 Past* 4, 47–57. doi:<hal-00330768>

654 Svensson, A., Andersen, K.K., Bigler, M., Clausen, H.B., Dahl-Jensen, D., Davies, S.M., Johnsen, S.J.,
 655 Muscheler, R., Rasmussen, S.O., Röhlisberger, R., Peder Steffensen, J., Vinther, B.M., 2006. The
 656 Greenland Ice Core Chronology 2005, 15–42 ka. Part 2: comparison to other records. *Critical
 657 Quaternary Stratigraphy* 25, 3258–3267. doi:10.1016/j.quascirev.2006.08.003

658 Tinner, W., Conedera, M., Ammann, B., Gaggeler, H.W., Gedy, S., Jones, R., Sagesser, B., 1998. Pollen
 659 and charcoal in lake sediments compared with historically documented forest fires in southern
 660 Switzerland since AD 1920. *The Holocene* 8, 31–42. doi:10.1191/095968398667205430

661 Türkeş, M., 1996. Meteorological Drought in Turkey: A Historical Perspective, 1930–93. *Drought
 662 Network News* (1994–2001) 84.

663 Tzedakis, P.C., 2007. Seven ambiguities in the Mediterranean palaeoenvironmental narrative. *Quaternary
 664 Science Review* 26, 2042–2066. doi:10.1016/j.quascirev.2007.03.014

665 Tzedakis, P.C., 2005. Towards an understanding of the response of southern European vegetation to
 666 orbital and suborbital climate variability. *Quaternary Science Reviews* 24, 1585–1599.
 667 doi:10.1016/j.quascirev.2004.11.012

668 Tzedakis, P.C., 1994. Hierarchical biostratigraphical classification of long pollen sequences. *Journal of
 669 Quaternary Science* 9, 257–259. doi:10.1002/jqs.3390090306

670 Tzedakis, P.C., Frogley, M.R., Lawson, I.T., Preece, R.C., Cacho, I., de Abreu, L., 2004. Ecological
 671 thresholds and patterns of millennial-scale climate variability: The response of vegetation in
 672 Greece during the last glacial period. *Geological Society of America* 32, 109–112.
 673 doi:10.1130/G20118.1

674 Tzedakis, P.C., Lawson, I.T., Frogley, M.R., Hewitt, G.M., Preece, R.C., 2002. Buffered Tree Population
 675 Changes in a Quaternary Refugium: Evolutionary Implications. *Science* 297, 2044–2047.
 676 doi:10.1126/science.1073083

677 Vanniere, B., Power, M.J., Roberts, N., Tinner, W., Carrión, J., Magny, M., Bartlein, P., Colombaroli, D.,
 678 Daniau, A.L., Finsinger, W., Gil-Romera, G., Kaltenrieder, P., Pini, R., Sadori, L., Turner, R.,
 679 Valsecchi, V., Vescovi, E., 2011. Circum-Mediterranean fire activity and climate changes during
 680 the mid-Holocene environmental transition (8500–2500 cal. BP). *Holocene* 21, 53–73.
 681 doi:10.1177/0959683610384164

682 Vigliotti, L., Channell, J.E.T., Stockhecke, M., 2014. Paleomagnetism of Lake Van sediments: chronology
 683 and paleoenvironment since 350 ka. *Quaternary Science Reviews* 104, 18–29.
 684 doi:10.1016/j.quascirev.2014.09.028

685 Wick, L., Lemcke, G., Sturm, M., 2003. Evidence of Lateglacial and Holocene climatic change and
 686 human impact in eastern Anatolia: high resolution pollen, charcoal, isotopic and geochemical
 687 records from the laminated sediments of Lake Van. *The Holocene* 13, 665–675.
 688 doi:10.1191/0959683603hl653rp

689 Wolff, E.W., Chappellaz, J., Blunier, T., Rasmussen, S.O., Svensson, A., 2010. Millennial-scale
 690 variability during the last glacial: The ice core record. *Vegetation Response to Millennial-scale*
 691 *Variability during the Last Glacial* 29, 2828–2838. doi:10.1016/j.quascirev.2009.10.013

692 van Zeist, W., Bottema, S., 1977. Palynological investigations in western Iran. *Palaeohistoria Bussum* 19,
 693 19–85.

694 Zohary, M., 1973. *Geobotanical Foundations of the Middle East*. Gustav Fischer Verlag, Swets &
 695 Zeitlinger. Stuttgart, Amsterdam.

696

697

698 Figures

699 Fig. 1: (A) Location of Lake Van in eastern Anatolia (Turkey) and (B) the bathymetry of Lake Van
 700 including the main ICDP drill site Ahlat Ridge (AR, black star). Major cities (black dots) and rivers are
 701 represented. The black triangle indicates the positions of the active volcanoes Nemrut and Süphan. The
 702 Bitlis Massif in the south reaches up to 3,500 m asl.

703 Fig. 2: Pollen diagram for the analyzed last glacial period from the Ahlat Ridge composite profile plotted
 704 against age (ka BP) and depth (event-corrected composite record; mcblf-nE). A 10-fold exaggeration line
 705 (gray) is used to show changes in low percentages. PAS – Pollen assemblage superzone; PAZ – Pollen
 706 assemblage zone. For the discussion see chapter 5.

707 (A) Shown is an arboreal/non-arboreal ratio (AP/NAP), selected arboreal pollen percentages (AP; gray),
 708 selected pollen concentrations (grains cm⁻³), microscopic charcoal concentration (>20µm; particles cm⁻³)
 709 and non-pollen palynomorph concentrations (NPP) such as *Pediastrum*, consisting of *Pediastrum*
 710 *boryanum* spp., *P. simplex*, and *P. kawraiskyi* (colonies cm⁻³), and dinoflagellate concentration (cysts cm⁻
 711 ³). (B) Shown is an arboreal/non-arboreal ratio (AP/NAP), selected non-arboreal pollen percentages (NAP;
 712 gray), and selected pollen concentrations (grains cm⁻³) of *Artemisia*, Chenopodiaceae, and Poaceae (red
 713 bars).

714 Fig. 3: Comparative study of the Lake Van palaeoenvironmental sequence encompassing the last glacial-
 715 interglacial cycle. (A) Mid-June and Mid-January insolation at 40°N (Berger, 1978; Berger et al., 2007);
 716 (B) Lake Van oxygen isotope record ($\delta^{18}\text{O}_{\text{bulk}}$ in ‰ PDB) of autochthonous precipitated carbonates.
 717 Shown is the temperature (T) and the isotopic composition ($\delta^{18}\text{O}_{\text{w}}$) of the epilimnion; (C)
 718 Calcium/potassium ratio (Ca/K) after Kwiecien et al. (2014); (D) Microscopic charcoal concentration
 719 (particles cm⁻³) from 10-110 ka BP (this study) and from 110-135 ka BP (MIS 5e; Pickarski et al. 2015);
 720 (E) Selected Lake Van arboreal pollen percentages (AP, *Pinus*, deciduous *Quercus*) from 10 and 110 ka

721 BP (this study) and from 110-135 ka BP described in Pickarski et al. (2015). MIS - Marine Isotope Stage;
 722 PAZ - Pollen assemblage zone.

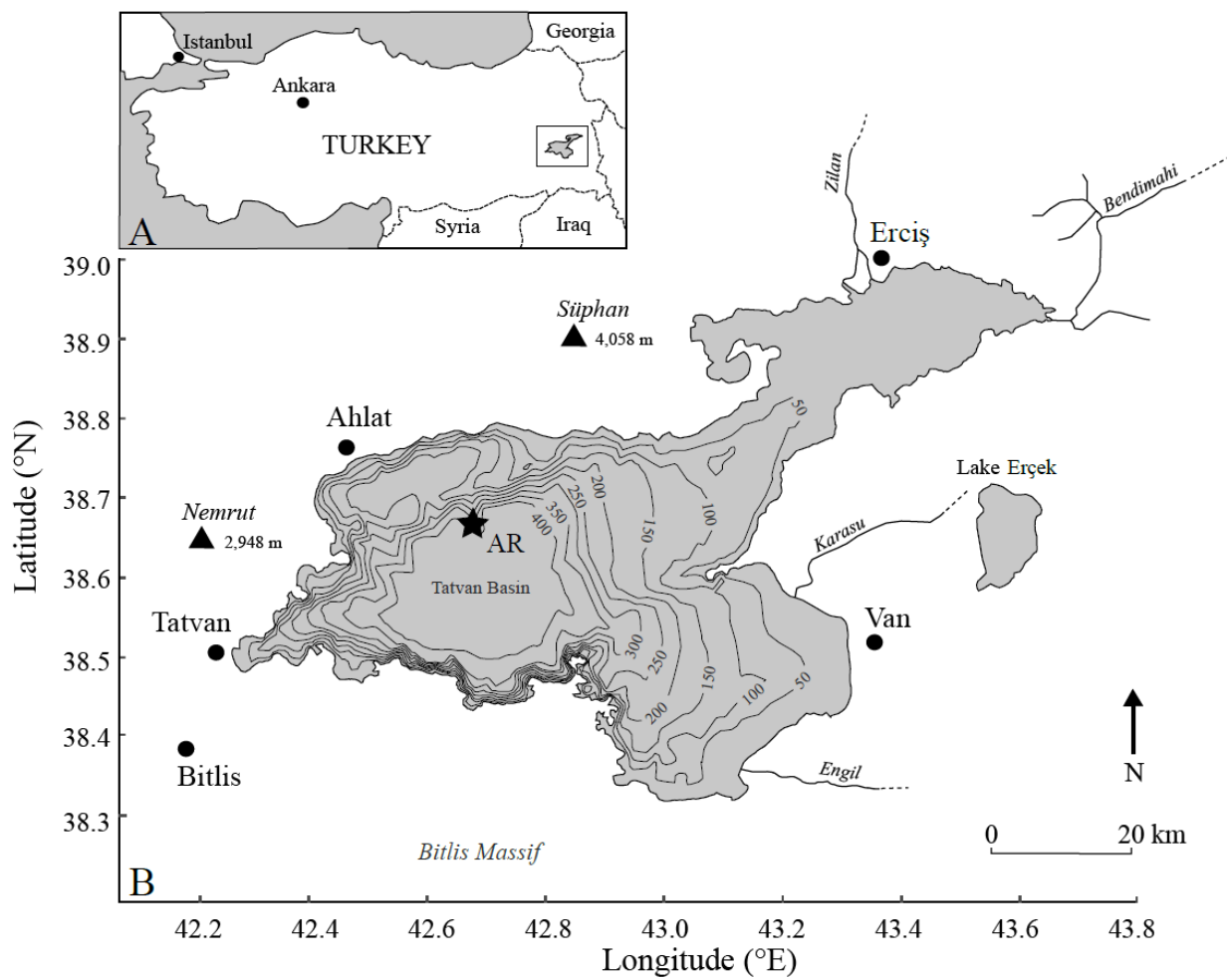
723 Fig. 4: Regional comparison of vegetation dynamics and climate variability in the central and eastern
 724 Mediterranean area and Black Sea region concerning Dansgaard-Oeschger cycles (DO) and Heinrich
 725 events (HE). (A) $\delta^{18}\text{O}$ -profile from NGRIP ice core, Greenland (NGRIP members, 2004), labelled with
 726 DO 1 to 19 and HE 1 to HE 6 (Bond et al., 1993); (B) Lake Van arboreal pollen record (AP in %, black
 727 line) with 1-fold exaggeration (gray line); (C) Marine arboreal pollen record (Core 9509) obtained from
 728 the south-eastern Levantine Basin (south-eastern Mediterranean Sea; Langgut et al., 2011); (D) AP record
 729 from the SE Black Sea (core 22-GC3 for the period from 10 to 18 ka BP after Shumilovskikh et al. (2012)
 730 and core 25-GC1 for the sequence between 19 and 63 ka BP (Shumilovskikh et al., 2014). (E) Arboreal
 731 pollen record from Tenaghi Philippon, Greece (Müller et al., 2011); (F) AP record from Lago Grande di
 732 Monticchio, southern Italy (Allen et al., 1999). MIS – Marine Isotope Stage.

733 Fig. 5: The longest Dansgaard-Oeschger events DO 8, DO 12, DO 14, DO 16-17 and DO 19 are plotted in
 734 extra graphs, demonstrating a good correlation between the vegetation and environmental dynamics in
 735 eastern Anatolia and the $\delta^{18}\text{O}$ -profile from the Greenland ice core sequences (NGRIP members, 2004);
 736 Ca/K ratio after Kwiecien et al. (2014); Microscopic charcoal concentration (particles cm^{-3} , this study);
 737 Selected Lake Van arboreal pollen (AP, *Pinus*, deciduous *Quercus* in %, this study). The term 'Steppic
 738 taxa' includes only major dry-adapted plants such as Chenopodiaceae and *Artemisia*.

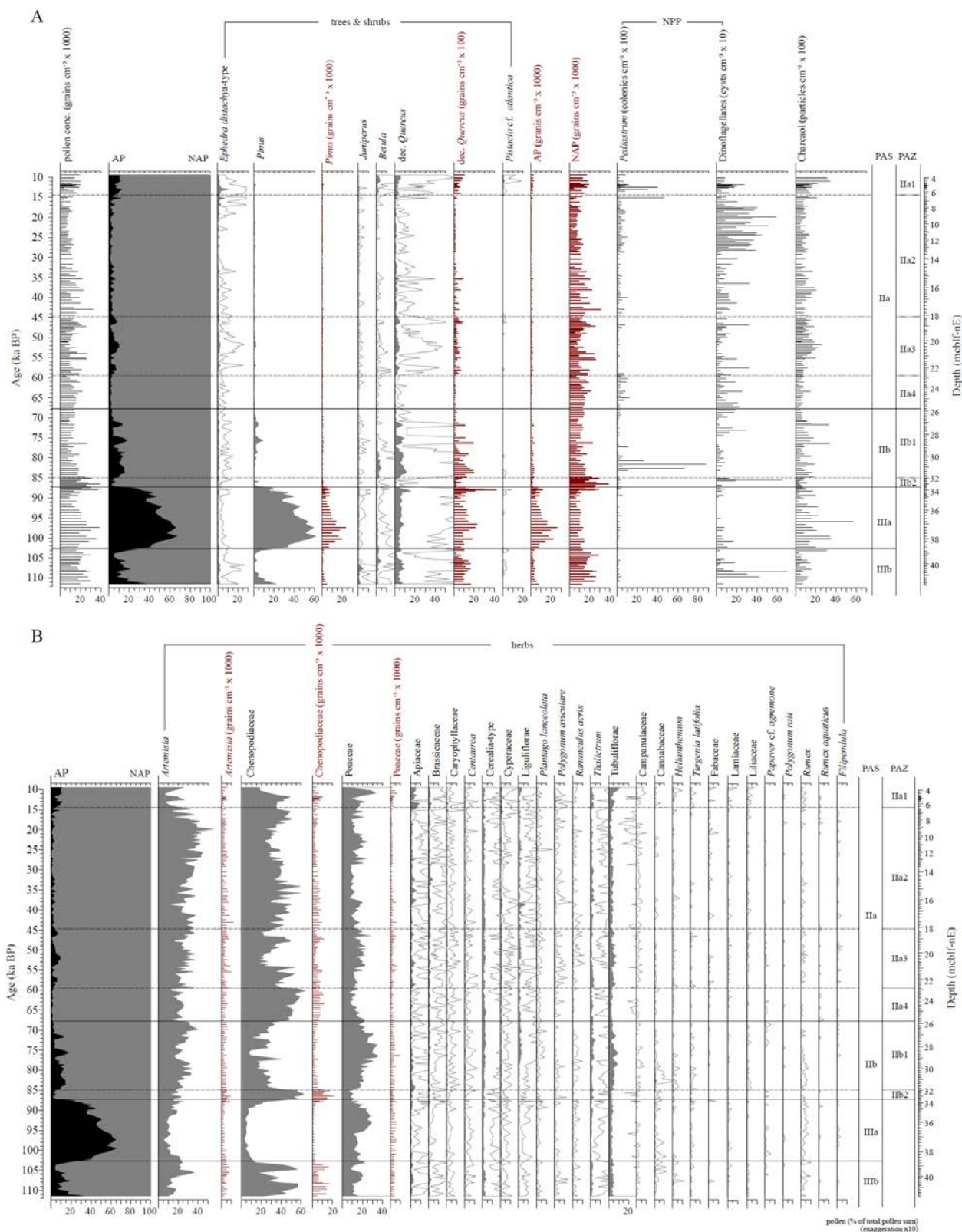
739 **Tables**

740 Table 1: Simplified synoptic description of pollen assemblage superzones (PAS) and zones (PAZ).

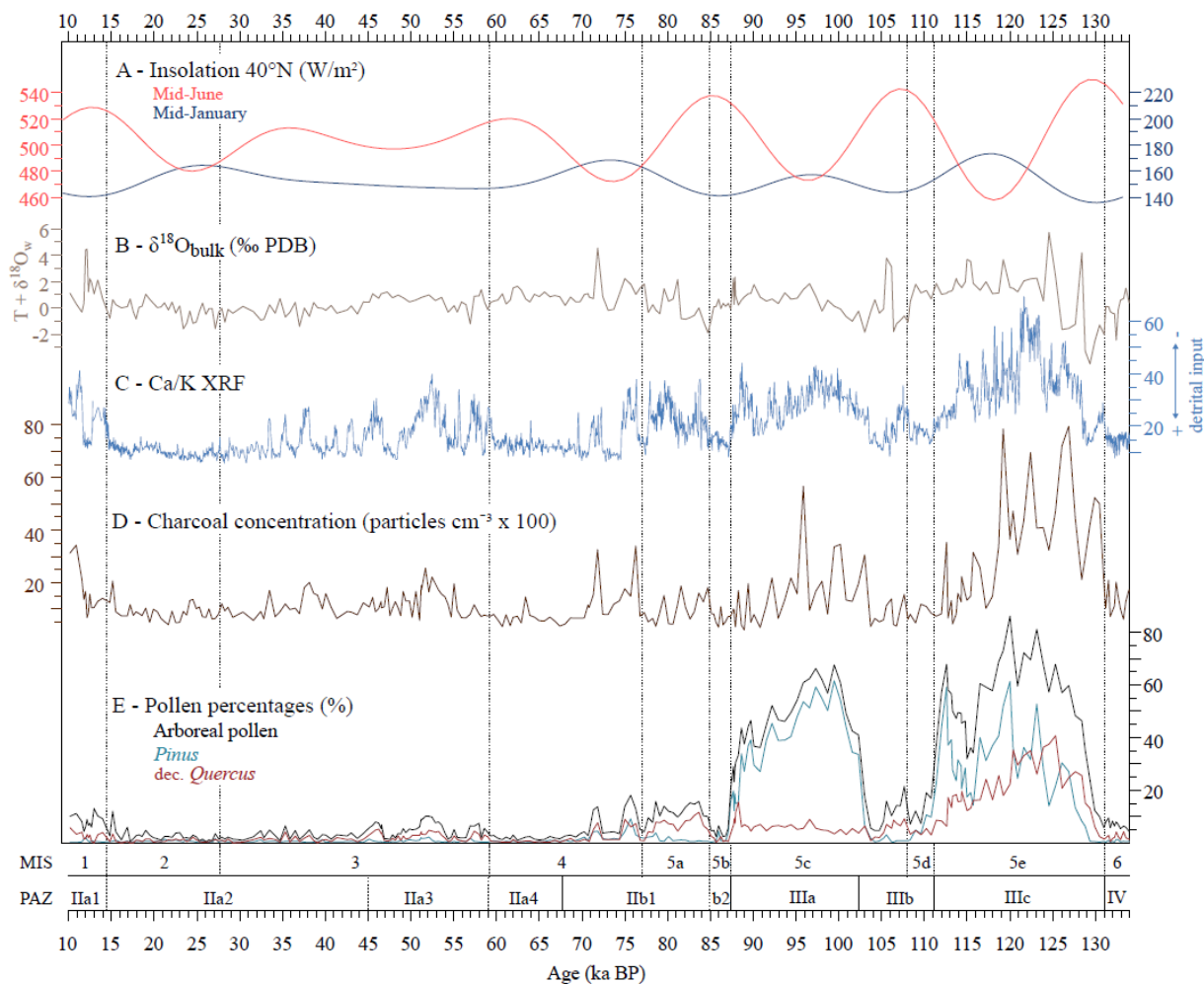
741 Fig. 1



742

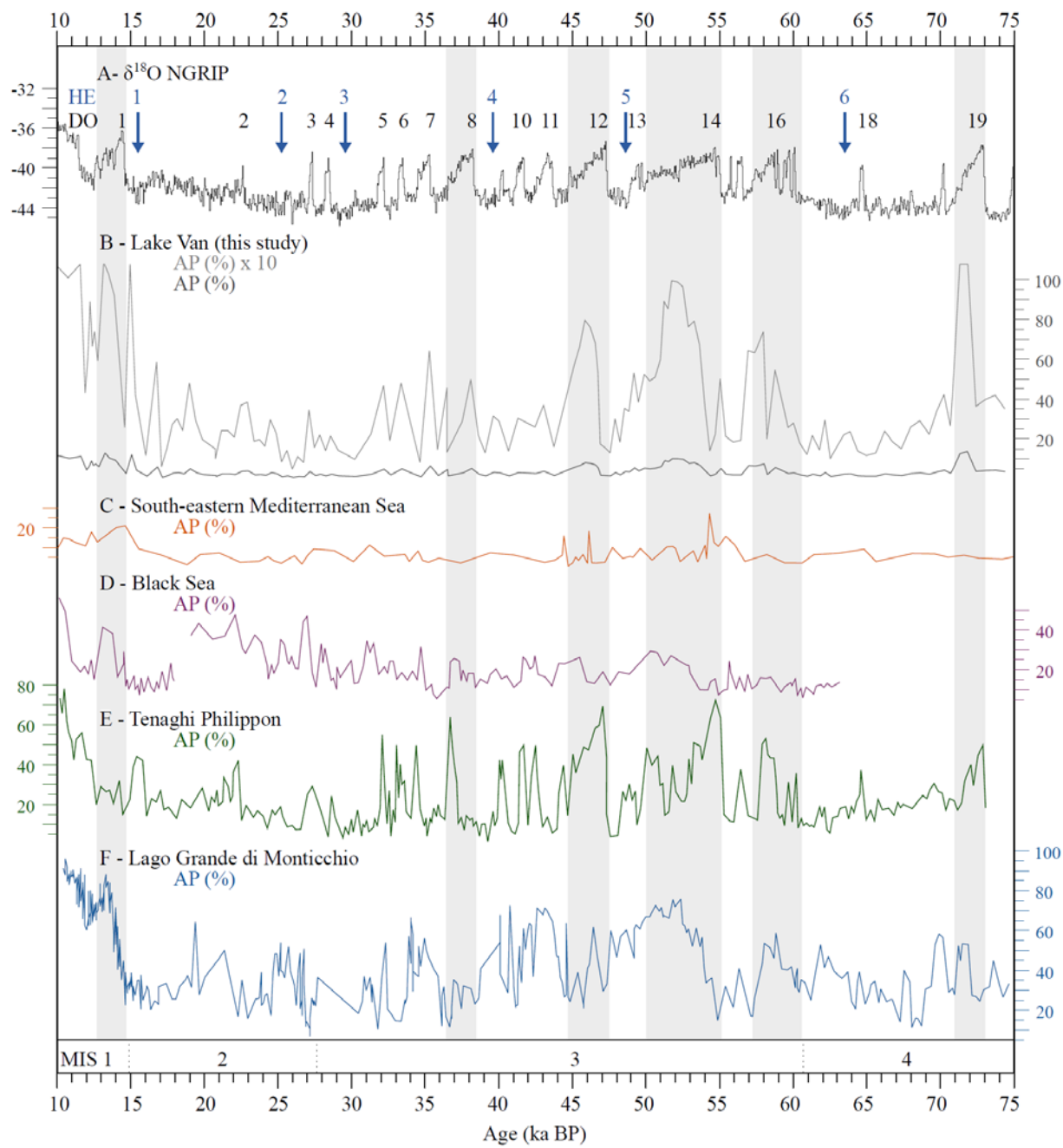


745 Fig. 3:



746

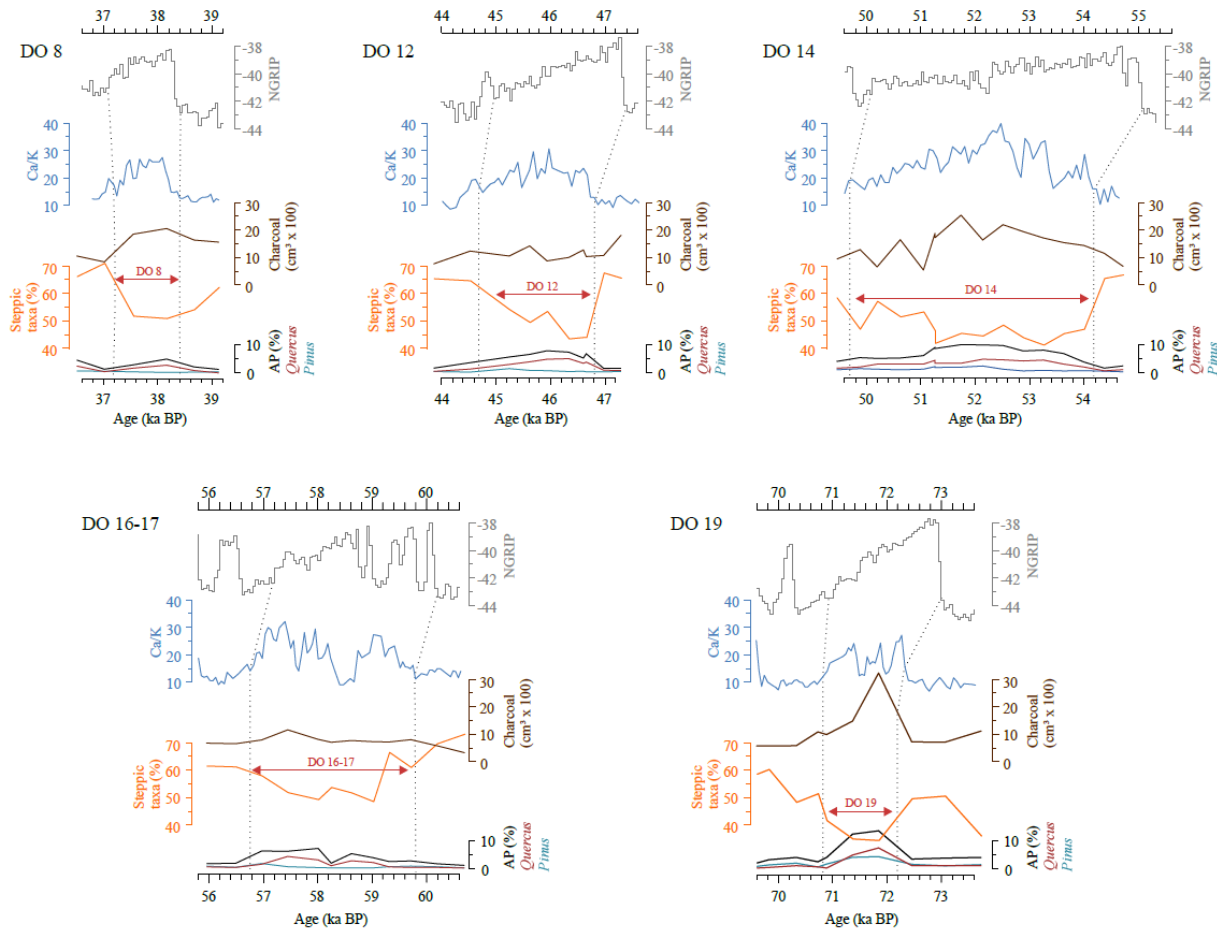
747 Fig. 4:



748

749 Fig. 5:

750



751

752 Table 1:

PAS/ PAZ	Age (ka BP)	Criteria for lower boundary	Pollen assemblages (minimum-maximum in %)
IIa1	09.48 - 14.26	Occurrence of <i>Pistacia</i> ; <i>Quercus</i> >3%	Chenopodiaceae (18-49%) - Poaceae (6-33%) - <i>Artemisia</i> (6-33%) - <i>Ephedra distachya</i> -type (1-11%) - dec. <i>Quercus</i> (0-6%) - <i>Betula</i> (0- 3%) - <i>Pistacia cf. atlantica</i> (0-2%) - <i>Juniperus</i> (0-1%) - <i>Pinus</i> (0-2%)
IIa2	14.26 - 44.80	<i>Quercus</i> <2%	Chenopodiaceae (23-60%) - <i>Artemisia</i> (10-55%) - Poaceae (7-26%) - <i>Ephedra distachya</i> -type (0-7%) - dec. <i>Quercus</i> (0-4%) - <i>Pinus</i> (0-2%) - <i>Betula</i> (0-1%)
IIa3	44.80 - 59.50	<i>Quercus</i> >2%; Chenopodiaceae <50%	Chenopodiaceae (15-57%) - <i>Artemisia</i> (12-37%) - Poaceae (10-28%) - dec. <i>Quercus</i> (0-5%) - <i>Ephedra distachya</i> -type (0-3%) - <i>Betula</i> (0- 2%) - Cyperaceae (0-2%) - <i>Pinus</i> (0-2%)
IIa4	59.50 - 67.72	Chenopodiaceae >50%	Chenopodiaceae (29-64%) - <i>Artemisia</i> (12-31%) - Poaceae (6-22%) - <i>Betula</i> (0-1%) - <i>Ephedra distachya</i> -type (0-1%) - <i>Pinus</i> (0-1%) - dec. <i>Quercus</i> (0-1%)
IIb1	67.72 - 84.91	<i>Quercus</i> >5%; Chenopodiaceae <50%	<i>Artemisia</i> (16-40%) - Chenopodiaceae (8-57%) - Poaceae (7-35%) - dec. <i>Quercus</i> (0-12%) - <i>Pinus</i> (0-9%) - <i>Betula</i> (0-5%) - <i>Ephedra</i> <i>distachya</i> -type (0-2%) - <i>Juniperus</i> (0-1%)
IIb2	84.91 - 87.24	<i>Pinus</i> <20%; Chenopodiaceae >50%	Chenopodiaceae (44-62%) - <i>Artemisia</i> (11-23%) - Poaceae (7-12%) - <i>Pinus</i> (0-16%) - dec. <i>Quercus</i> (0-4%) - <i>Betula</i> (0-1%) - <i>Ephedra</i> <i>distachya</i> -type (0-1%)
IIIa	87.24 - 102.67	<i>Pinus</i> >20%; Chenopodiaceae <20%	<i>Pinus</i> (7-61%) - Poaceae (8-29%) - <i>Artemisia</i> (5-25%) - Chenopodiaceae (3-50%) - dec. <i>Quercus</i> (3-15%) - <i>Betula</i> (0-2%) - <i>Alnus</i> (0-1%) - <i>Ephedra distachya</i> -type (0-1%) - <i>Juniperus</i> (0-1%) - <i>Pistacia cf. atlantica</i> (0-1%)
IIIb	102.67- 111.70	Chenopodiaceae >20%	Chenopodiaceae (14-57%) - Poaceae (8-22%) - <i>Artemisia</i> (7-36%) - dec. <i>Quercus</i> (1-9%) - <i>Pinus</i> (0-22%) - <i>Juniperus</i> (0-5%) - <i>Betula</i> (0- 4%) - <i>Ephedra distachya</i> -type (0-3%) - <i>Fraxinus</i> (0-1%) - <i>Pistacia cf.</i> <i>atlantica</i> (0-1%)